ADVANCED HEALTHCARE MATERIALS
www.advhealthmat.de

Electronic Neurons for a New Learning Paradigm

*Zhen Wang, Jiajia Wang, Xiang Shi, Zhengfeng Zhu, Peining Chen, and Huisheng Peng**

Learning is the cornerstone of the growth and development of human beings. However, traditional learning methods are insufficient to meet the explosive growth of knowledge and information. Repeated training accounts for a large proportion of learning time, which significantly limits the improvement of learning efficiency. Inspired by cloud storage technology, electronic neurons (E-neuron) with functions similar to neurons in the brain are proposed. Implanted E-neurons can form new patterns of neural activity in circuits, including both E-neurons and biological neurons, which can transfer knowledge from electronic cloud devices to human beings without training. Herein, the feasibility of this concept is preliminarily demonstrated. Fiber neural electrodes (FNEs) made of poly(3,4-ethylene dioxythiophene) (PEDOT) modified carbon nanotubes (CNTs) are used to form both dendrites and axons of E-neuron. After the implantation of an E-neuron in a mouse's brain, an electrical neural connection is created between the mitral cell and dorsolateral periaqueductal gray (dlPAG). A piece of knowledge similar to "The red light stops; the green light is all right." is then passed on to the mouse.

1. Introduction

From the emergence of animals on the earth to the evolution of humans for thousands of years, the typical learning model is that organisms receive external information through the senses and perform repeated training before they can gradually memorize and accumulate knowledge.[1–4] The nature of knowledge is mainly summarized as the generation of new synaptic connections and the formation of new patterns of neural activity in neural circuits, which is time-consuming and requires degrees of training.[5–8] Even for human beings, the knowledge learned is very limited in decades of life. Therefore, traditional learning efficiency needs to be more efficient for human beings when facing the explosive growth of knowledge and information, which severely limits the development of science and technology.

In recent years, different kinds of artificial neurons were established.[9,10] They show highly similar functions to biological neurons. Memristors and organic transistors used in these artificial neurons acted mainly as their signal processing units. However, few memristors or transistors were used in artificial neurons, so their processing capacity was restricted, especially facing complicated signals in the brain. Inspired by cloud storage technology, which can share massive amounts of information between electronic devices in seconds,[11,12] we propose an E-neuron capable of implanting knowledge from electronic cloud devices. Similar to neurons in the brain, E-neuron has functional modules consisting of receiving, processing, and sending (**Figure 1**). The dendrites and axons of implanted E-neurons were both made of conducting electrodes and directly participated in brain operation. As the processing core of the E-neuron, the electronic cell body is a processing and judging program stored in electronic cloud devices. It will selectively and precisely link two groups of specific functional cells with electronic dendrites and axons based on particular knowledge. New knowledge exists in the form of a unique pattern of neural activity in neural circuits composed of both E-neurons and biological neurons. Such a process is expected to promote a new learning paradigm in which E-neurons become the bridge between cloud knowledge and the brain. It is foreseeable that large amounts of knowledge will be able to be transferred from the cloud to human beings to realize the sharing of knowledge when this type of E-neuron system is sufficiently connected with the brain.

Here, we illustrated an elementary knowledge implantation example to demonstrate the feasibility of this concept. "The red light stops; the green light is all right." is a widely known knowledge for traffic safety in the human world. Nevertheless, a preschool child must be repeatedly taught to acquire this knowledge, let alone a mouse.[13,14] But now, through the implanted E-neurons, a similar knowledge like "Sharp smell stops; the mild smell is all right." was passed on to mice without training.

In this study, an E-neuron connection was created between the mitral cell and dorsolateral periaqueductal gray of mice. Fiber neural electrodes made of PEDOT-modified CNTs were used as both the dendrites and axons of E-neuron to obtain sufficient implanting depth and working stability and quality. Low specific impedance, together with high charge storage capacity, was acquired by fiber neural electrodes simultaneously.

As the processing core of the E-neuron, the electronic cell body is a computer program that is responsible for calculating the

Z. Wang, J. Wang, X. Shi, Z. Zhu, P. Chen, H. Peng
Laboratory of Advanced Materials
State Key Laboratory of Molecular Engineering of Polymers, and
Department of Macromolecular Science
Fudan University
Shanghai 200438, P. R. China
E-mail: penghs@fudan.edu.cn

The ORCID identification number(s) for the author(s) of this article can be found under https://doi.org/10.1002/adhm.202203247

DOI: 10.1002/adhm.202203247

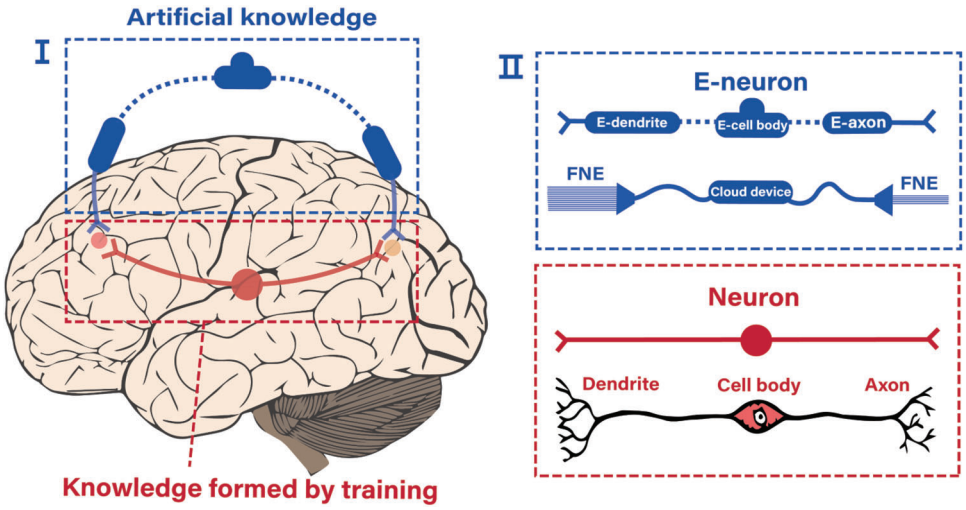

Figure 1. I) Mechanism comparison between artificial knowledge formation and traditional knowledge formation. II) Comparison between E-neurons and brain neurons.

firing rate and triggering subsequent firing when it reaches the pre-set threshold. Here, the electronic cell body could wirelessly connect to the E-dendrites and E-axons.

2. Results and Discussion

Stable interneural connections and efficient electrochemical signal transmission are the basis for the operation of neurons.[15–17] Hence, an excellent electrode-brain interface, high recording quality, and stability of electronic dendrites and axons are the essential parts of E-neurons. As a flexible material with high electronic properties,[18–21] twisted CNT fibers have been selected as the conduction backbone of electronic dendrites and axons. PEDOT: PSS was used as a modification layer to enhance its electronic interface properties further to reduce its interface impedance and increase charge storage capacity.[22] Polyvinylidene fluoride-hexafluoropropylene (PVDF-HFP), a good insulating material with high biocompatibility, was chosen to fabricate the insulation layer of the fiber neural electrode. Fiber neural electrodes were ~20 μm in diameter with coaxial structure, where PVDF-HFP, PEDOT: PSS and twisted CNT fiber was used as the insulation layer, modification layer, and conductive core, respectively (**Figure 2**a). Detailed observations revealed that the conduction backbone of fiber neural electrodes consisted of twisted clusters of aligned CNTs (Figure 2a), which secured the excellent conductivity of fiber neural electrodes.

A low interface impedance will provide a high signal-to-noise ratio for an electrode with a given size, greatly benefiting its recording quality.[23] Moreover, the specific impedance determines the minimum allowable size of the electrode.[24] Here, PEDOT-modified fiber neural electrodes had specific impedances as low as 7097 kΩ·μm^2 (at 1 kHz, Figure 2b), which were lower than most reported neural electrodes, such as bare CNT electrodes (33 873 kΩ·μm^2 at 1 kHz) and tungsten electrodes (455 546 kΩ·μm^2 at 1 kHz, Figure 2b). Thus, the electrode size could be small enough (20 μm in diameter), which not only ensured the specificity of the electronic dendrites' recording signal and improved the charge-injecting resolution of electronic axons.

The electrodes showed good electrochemical stability, and no obvious variation was observed after 1000 cycles of cyclic voltammetry test (Figure 2c). At the same time, the electrochemical performance showed an excellent consistency among ten fiber neural electrodes prepared in the same batch (Figure 2d and S1). Furthermore, high charge storage capacity can also improve the quality of neural recordings.[25] Fiber neural electrodes showed a high charge storage capacity of 1808 mC·cm^{-2} (Figure S2a), which is much higher than other neural electrodes, such as PtIr wires (6 mC·cm^{-2}), CNT fibers (316 mC·cm^{-2}) and stainless-steel wires (231 mC·cm^{-2}, Figure S2b–d).

A single fiber neural electrode was then implanted into the mouse olfactory bulb's plexiform and mitral cell layer as electronic dendrites to verify its recording performance in vivo and olfaction-sensing ability (**Figure 3**a). Firstly, signals were recorded in an anesthetized mouse during the switch of odor stimulation (isoamyl acetate). A significant difference in the action potential firing rate was observed (Figure 3b). The collected firing rate when smelling the odorant (~86 spikes·50s^{-1}) was significantly higher than the firing rate of the odorless substance (~11.5 spikes·50s^{-1}). The p-value between the two circumstances was less than 7×10^{-5} through the student's t-test (n = 4, Figure 3c). Additionally, the high recording quality brought about by the low impedance and large charge storage capacity enabled electronic dendrites to record consistent action potentials of a single type (Figure 3d and S3a). The pure signal recording laid the foundation for the program analysis of firing rates.

To further verify the capability of fiber neural electrodes in collecting neural signals when it was used as electronic dendrites, neural signals of different concentrations of odorant (isoamyl acetate) were then immediately recorded in the anesthetized mice, and a clear trend in firing rate was also observed (Figure 3e). When the odor concentration decreased from 10^{-1} to 10^{-5} mol/L, a noticeable decrease (86 to 23.8 spikes·50s^{-1}) was observed in the average firing rate of the neuron recorded (Figure 3f).

Restricted by technical conditions, electrical stimulation electrodes were tentatively used for the electronic axons to excite subsequent nerves in this study (Figure 3g). More precise and

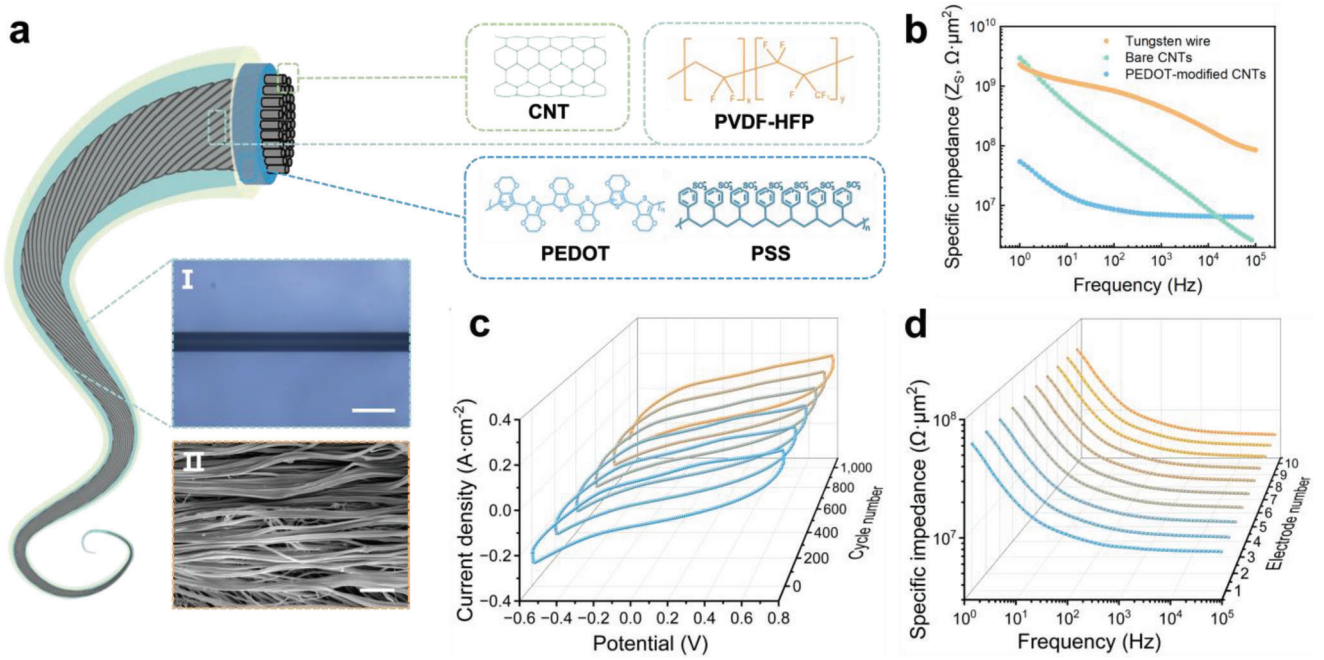

Figure 2. a) Schematic diagram of the coaxial structure of the electrode. Twisted CNT fiber, PEDOT: PSS layer and insulation layer from the inside out. I. Optical microscope photograph of fiber neural electrode without an insulation layer, scale bar: 40 μm. II. Scanning electron microscope image of the surface of twisted CNT fiber, scale bar: 500 nm. b) Specific impedance spectroscopy of tungsten wire, bare CNT fiber, and PEDOT-modified CNT fiber. c) Representative CV curves of specific cycle number in 1000 CV cycles (scan rate: 0.1 V/s). d) Specific impedance spectroscopy of ten fiber neural electrodes prepared in the same batch.

non-destructive neuron stimulation methods are expected to play a better role of the electronic axon in future work, such as optogenetics.[26,27]

As a nerve electrode with high electrical conductivity, a fiber neural electrode can also be used as an electrical stimulation electrode. Three juxtaposed fiber neural electrodes were used as electronic axons and implanted into the dorsolateral periaqueductal gray (dlPAG) to verify their ability to guide mouse behavior when used as electronic axons (Figure 3g,h). Among the three electrodes, two were used as stimulation and counter electrodes, and the third electrode was a backup. After implantation, mice can move freely without electrical input. Under the condition that the pulse width (1 ms), train period (2.5s), and train width (1.5s) remained unchanged, a monophasic electrical stimulation train with different pulse periods was put into the electronic axon, and it could be observed that the behavioral freezing time of mice increased significantly as the pulse period shortened. The mouse can remain still for 39.7s on average when the pulse period was 10 ms (n = 8, Figure 3i). The mouse tried to escape when the pulse period of the stimulus train was smaller than 5 ms. Therefore, a pulse period of 15 ms was used in the following experiments, which was moderate enough to only lead to the freezing behavior of the mouse.

As an example of elementary knowledge, a neural signal analysis program and a simple judgment code were used as the cell body of the E-neuron (**Figure 4**a). The neural signals were first denoised and filtered through the electronic cell bodies. A simple judgment program was used to calculate the firing rate of received neural signals in real-time. Once the calculated rate was higher than a pre-set threshold, which means the mice smelled a sharp odor, the program would automatically release a predetermined electrical stimulation train to the electronic axon and guide the freezing behavior of mice.

An electronic trigger was used to control the functioning of the E-neuron. When the trigger was inactivated, the electronic cell body would not send an electrical stimulation train to the electronic axon under any circumstance. In this case, the mouse was implanted with blank pieces of knowledge. When the trigger was activated, each input neural signal sent by the electronic dendrites would be put into the electronic cell body and trigger the sending of predetermined electrical stimulation train according to different situations. In this case, rudimentary knowledge was implanted into the mouse brain (Figure 4a).

Since the awake-state firing rate received by the electronic dendrites while mice sniffing an odorous object (~49.3 spikes·s^{-1}) was significantly higher than the state while sniffing environmental odor (8.3 spikes·s^{-1}, n = 4, p-value: 8.4×10^{-4}, Figure 4b,c, S3b, and S4), the threshold of the electronic cell body was set to be 20 spikes·s^{-1}. This means, once the calculated firing rate was higher than 20 spikes·s^{-1}, the electronic cell body would immediately release the electrical stimulation train to the electronic axon. The electrical stimulation train sent by the electronic axon to dorsolateral periaqueductal gray was set to have a pulse period of 15 ms with a train period of 1.5 s (Figure 4a and S5).

Finally, a complete E-neuron was assembled and implanted in the mouse brain, connecting the cell in the mitral layer to the dorsolateral periaqueductal gray (Figure 4d). In this E-neuron, the electronic dendrites prepared by fiber neural electrodes exhibited high recording quality of the mitral cell layer. The electronic cell body showed the preliminary perception ability

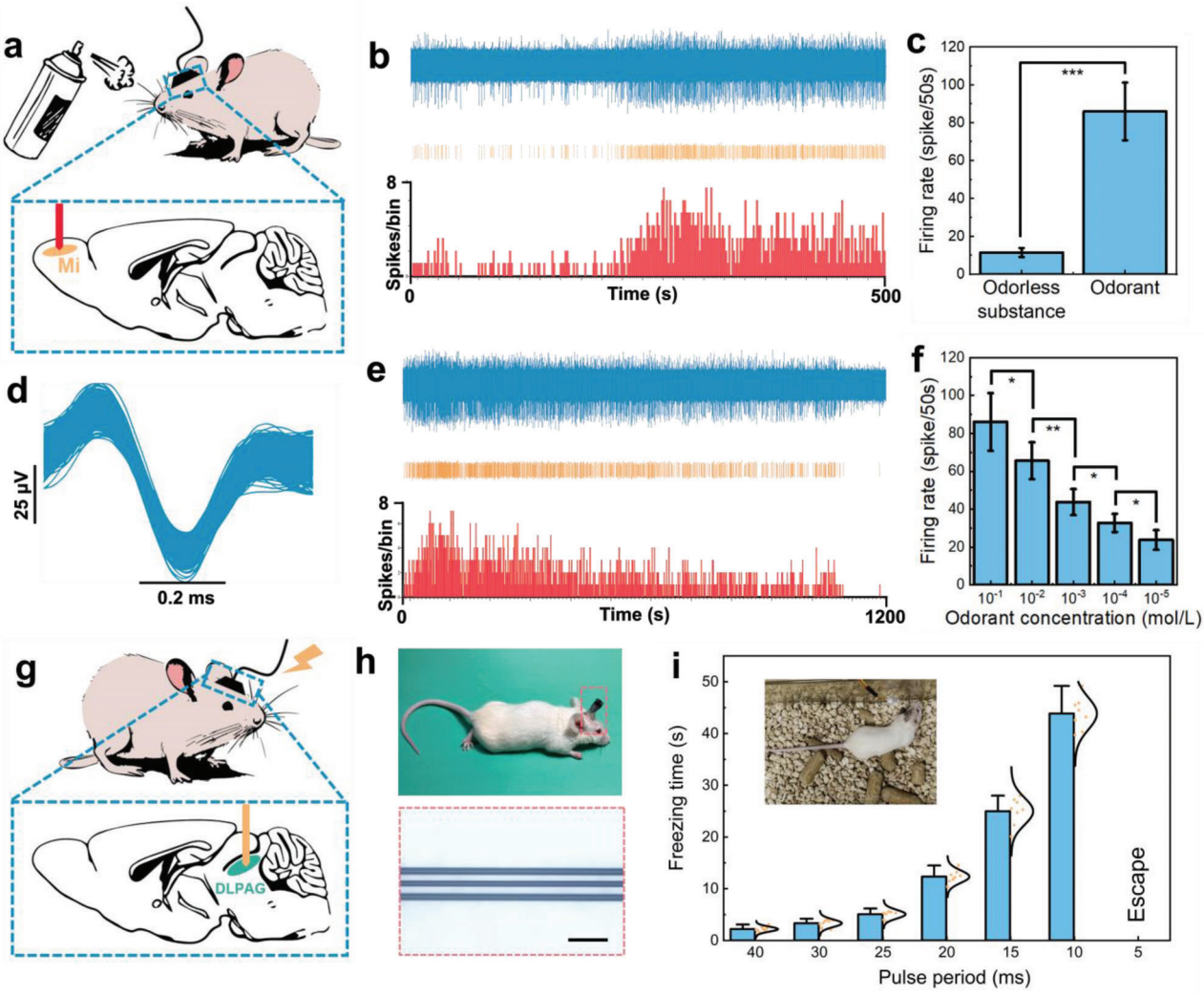

Figure 3. a) Schematic diagram of a single fiber neural electrode implanted into the mitral cell layer of the mouse olfactory bulb as electronic dendrites. b) Recording of mitral cells in anesthetized mice during the switch of odor stimulation. Signal in blue: the denoised neural signal received by the E-dendrite; signal in orange: the action potential sorted from the raw signal; statistics in red: the frequency statistics of the action potential per unit time. c) Statistics on firing rate during the switch of odor stimulation (n = 4, p-value: 7×10^{-5}). d) Waveforms from the recorded mitral cell. e) Recording of mitral cells in anesthetized mice during different concentrations of odor stimulation. f) Statistics on firing rate during different concentrations of odor stimulation (n = 4, p-values: 0.03, 0.005, 0.02, and 0.02). g) Schematic diagram of three juxtaposed fiber neural electrodes used as electronic axons and implanted into the dorsolateral periaqueductal gray (dlPAG). h) Photographs of mice after implantation and optical microscope image of juxtaposed fiber neural electrodes, scale bar: 100 μm. i) Statistics on freezing time increasing as pulse period shortened from 40 to 5 ms. $^*P < 0.05$, $^{**}P < 0.01$, $^{***}P < 0.001$.

of the mouse olfactory sense in distinguishing mild or sharp smells and triggering the electronic axon at the sharp smell. Fiber-neural-electrode-prepared electronic axons could correspondingly and effectively stimulate subsequent neurons and guide the freezing behavior of mice.

It can be observed that the mice's perception of environmental odors (odorless objects) and odorous objects existed only in the difference of smell when the E-neuron was not activated (Figure 4e). Mice tended to avoid the odorant, which was the same as before the E-neuron implantation. When the trigger was activated, the mice responded significantly differently to the two different odors (Figure 4f). After smelling the odorant, the mice showed apparent freezing behavior; while under the environmental odor, the mice could still move freely. Through the student's t-test, the p-value between the two circumstances was less than 2×10^{-11} (n = 8). As a result, a knowledge similar to "The red light stops; the green light is all right." was conveyed to the mice: "The sharp smell stops; the mild smell is all right." Additionally, this knowledge existed only when E-neurons were engaged.

3. Conclusion and Perspective

In conclusion, inspired by cloud storage technology, we propose using E-neurons as a part of the brain to transfer cloud knowledge to human beings. In this regard, we preliminarily designed an E-neuron to test our idea, using a PEDOT-modified CNT fiber neu-

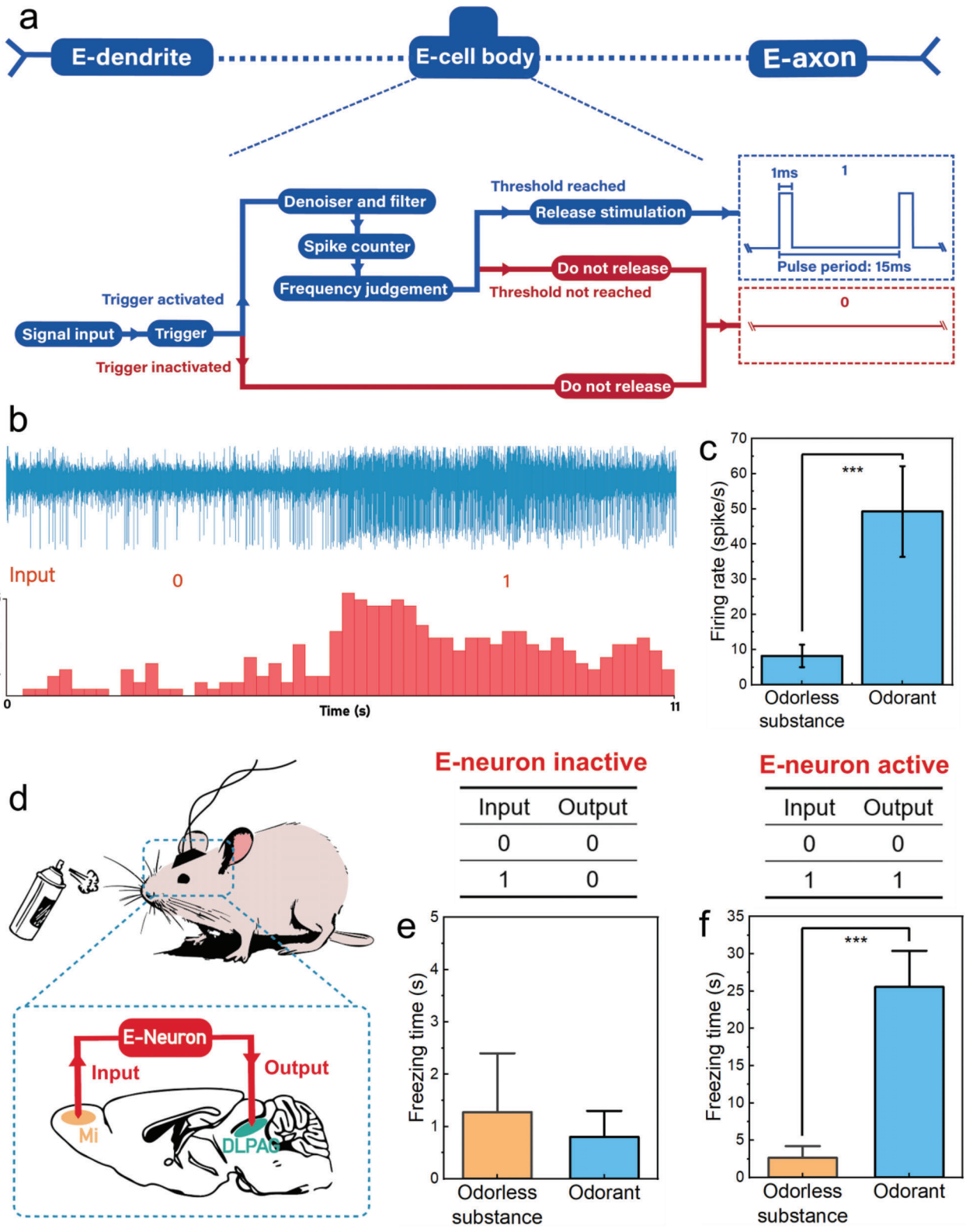

Figure 4. a) Schematic diagram of signal judgment and processing process inside the cloud electronic cell body. b) Recording of mitral cells in a free-moving mouse during the switch of odor stimulation. Signal in blue: the denoised neural signal received by the E-dendrite; statistics in red: the frequency statistics of the action potential per unit time. c) Statistics on firing rate during the switch of odor stimulation (n = 4, p-value: 8.4×10^{-4}). d) Schematic diagram of E-neuron implantation. e) Statistics on freezing time of the control test when E-neuron was inactive (n = 8). f) Statistics on freezing time when E-neuron was active (n = 8, p-value: 2×10^{-11}). $^{*}P < 0.05$, $^{**}P < 0.01$, $^{***}P < 0.001$.

Figure 5. Schematic of transferring and sharing knowledge by E-neurons.

ral electrode with low specific impedances and high charge storage capacitance as electronic neural dendrites and axons. Electronic cell bodies could effectively distinguish the mouse's olfactory sense of mild or sharp smells and trigger the following electronic axon when it was a sharp smell. After implanting E-neurons into mice, a rudimentary piece of knowledge was implanted. Furthermore, we showed that this knowledge existed only when E-neurons were engaged.

Of course, this technology is still at a very early stage. The implantation of complex/advanced knowledge not only requires the co-implantation of multiple or even a large number of E-neurons but also relies on extensive and stable neural signal acquisition,[28–30] efficient and intelligent neural signal analysis,[31–33] and precise and non-destructive neuron excitation/stimulation.[34] In the initial stage, this technology will focus on the repair of fundamental brain reflection; for example, it will help patients with cerebral infarction and Alzheimer's disease regain their body balance and self-care ability. We believe, with the further development of sensing devices, this technology may become a general and effective strategy to transfer a large amount of knowledge from the cloud to humans and realize the sharing of knowledge among different people (**Figure 5**), thereby, significantly improving the learning efficiency and intelligence level of human beings.

4. Experimental Section

Preparation of CNT Fibers: The CNT fibers were synthesized via floating catalyst chemical vapor deposition with thiophene (1–2 wt.%) and ferrocene (1–2 wt.%) as the catalyst. Flowing ethanol (> 97 wt.%), Ar (200 sccm), and H_2 (2000 sccm) were used as carbon source, carrier gas, and reduction gas, respectively. The CNT aerogel was produced continuously at the hot zone of a tube furnace with a reaction temperature of 1200 °C, then collected into cylindrical hollow socks. The CNT sock was pulled out of the furnace by a titanium rod and then densified through water and ethanol in turn. The CNT sock shrank immediately into the CNT ribbon upon arriving at the water's surface. It was finally washed with acetone for further densification, followed by drying, twisting, and collecting onto a spool to produce CNT fibers. By controlling the twisting and collection speed, CNT fibers were produced with designed specific diameters (typical diameter of 15 µm).

Preparation of Fiber Neural Electrodes: PEDOT: PSS aqueous solution (PH1000, Heraeus) was placed on a hot table with a stirring speed of 100 rpm until it was concentrated to a solid content of 2.5%. 5 wt.% dimethyl sulfoxide (DMSO, Sinopharm Chemical Reagent Co., Ltd) was added to the concentrated solution, and then stirred for 2 h, and filtered. A bubble removal process was carried out in a vacuum oven. CNT fibers would go through an oxygen treatment before the dip coating process of the PEDOT: PSS layer to make the surface hydrophilic.

Fluor rubber (PVDF-HFP G801) was dissolved in 4-methyl 2-pentanone (Sinopharm Chemical Reagent Co., Ltd) with a mass fraction of 20%. Fiber neural electrodes were finally obtained by a dip-coating process at a constant speed. Good ventilation was ensured during the process, so the quick solvent evaporation could avoid the Plateau-Rayleigh instability.

Morphological and Elemental Characterization: The optical image was captured by Olympus EX51. Scanning electron microscopy (SEM) images were obtained by Zeiss Gemini SEM500 FESEM. A freeze dryer was used to prepare samples for SEM imaging.

Electrochemical Characterization: Electrochemical characterization was characterized by an Electrical workstation (CHI660E, CH Instruments Ins.). The test electrode (i.e., fiber neural electrode) was used as the working electrode, with the reference electrode of Ag/AgCl, and the counter electrode of platinum wire. PBS (0.01 M, pH = 7.4) was used as the electrolyte. Impedance and cyclic voltammograms were measured by the impedance function and CV function respectively. The electrode diameter was measured by Olympus EX51 and the electrode length was measured by a vernier caliper.

In Vivo Electrophysiology: A 2 × 10 pin connector was used for the adapter of fiber neural electrodes and connected by silver glue. Sealed the joint with silicone rubber for EMI mitigation. Gelatin was added to water with a mass fraction of 30% and stirred at 159 °C to form a viscous solution. For assistive implantation, gelatin fibers with a diameter of 10 µm were fixed on the connector, paralleling to the electrodes. PEG 4000 was melted at 120 °C and used to bond them. Before implantation, disinfection with ultraviolet radiation was performed on a clean bench.

Fiber neural electrodes were tested in mice (ICR, 6 weeks old, Shanghai SLAC Laboratory Animal Co., Ltd.) housed in an ordinary animal room (12 h light/dark cycle, 22 °C, food, and water ad libitum). Surgeries were performed on deeply anesthetized mice positioned in a stereotactic frame (RWD). Mice were pretreated with atropine sulfate (0.1 mg per kg, intraperitoneally), and anesthetized with chloral hydrate (400 mg per kg). Then the scalp was removed by scissors. An electric drill was used to remove the skull of implantation sites. The adaptor with electrodes was loaded into an FHC hydraulic micro-positioner (FHC INC).

The skull was drilled with a hole about 2 mm in diameter by using a skull drill with the following stereotaxic coordinates: anteroposterior (AP), 4.6 mm; mediolateral (M/L), 0.8 mm for mitral cell layer and anteroposterior (AP), -4.7 mm; mediolateral (M/L), 0.5 mm for dlPAG layer. A sterile syringe needle was used to remove the dura mater. A flat head screw was screwed to another side as ground and reference. Electrodes were implanted at a depth of 200 µm and 1.9 mm below the cortex.

For mice in chronic test, bare brain tissue was covered with a layer of agarose gel (1 wt.%) after implantation, then with a layer of paraffin, and finally fixed to the skull with a dental resin adhesive (Super Bond C&B, SUN MEDICAL). After the dental resin adhesive had been completely solidified, iodophor was applied around the wound. All surgical instruments were sterilized. Cefuroxime sodium (2 mg kg^{-1}) was administered subcutaneously over the shoulders to reduce the inflammatory response,

followed by the subcutaneous administration of 0.5% lidocaine directly under the scalp incision site.

In the acute test, the electrophysiological recording was performed immediately. Isoamyl acetate (Sigma-Aldrich) was used as an odorant and the clean air was used as the odorless substance. The odorant was diluted in mineral oil in different concentrations and stored in light-shielded vials. Before use, the odorant (50 µL) was placed on filter paper and put in front of the mouse's nose. The raw data were collected through BlackRock Microsystems. Offline analysis was performed using Spike 2 (CED).

In the chronic test, the electrophysiological recording was performed on mice after recovery for one week. Mice were placed in their familiar environments without moving restrictions. The raw data were collected through BlackRock Microsystems. The firing rate was analyzed in real-time by the program. The stimulation train was preset and given by MODEL 3800. Offline analysis was performed using Spike 2 (CED).

Approval Statement: All the animal experimental procedures were approved by the Ethics Committee of Fudan University (Approval number: SYXK2020-0032) and the International ethical guidelines and the National Institutes of Health Guide concerning the Care and Use of Laboratory Animals were strictly followed.

Statistical Analysis: The raw data were collected through BlackRock Microsystems. Raw data were pre-processed through a high-pass filter with a passing frequency range of 800—5000 Hz. Offline analysis was performed using Spike 2 (CED). Action potentials were sorted through its spike sorting function with a threshold of ±25 µV. All images were confirmed by at least three independent experiments with similar results. All data were shown in mean corrected values ± S.D. of at least four independent experiments unless otherwise stated. Graphing of the data was conducted using Microsoft Office Excel, Origin 2022, and Adobe Illustrator CC 2018. Except for the data in Figure 3f, all statistical analyses were performed using a two-tailed student's t-test with a sample size of at least 4 ($n = 4$). In Figure 3f, statistical analyses were performed using a one-tailed student's t-test with a sample size of 4 ($n = 4$). $p < 0.05$ was considered significant ($^*p < 0.05$, $^{**}p < 0.01$, and $^{***}p < 0.001$; n.s., not significant). All results are presented as the mean ±standard deviation (S.D.).

Supporting Information

Supporting Information is available from the Wiley Online Library or from the author.

Acknowledgements

This work was supported by the Science and Technology Commission of Shanghai Municipality (20JC1414902, 21511104900) and the China Postdoctoral Science Foundation (VLH1717003, KLH1717015). The authors thank C. Tang, X. Sun, L. Wang, K. Zhang, and Z. Liu for their assistance.

Conflict of Interest

The authors declare no conflict of interest.

Data Availability Statement

The data that support the findings of this study are available from the corresponding author upon reasonable request.

Keywords

carbon nanotubes, electronic neurons, neural electrodes, new learning paradigm, polymers

Received: December 15, 2022
Revised: February 23, 2023
Published online: April 10, 2023

[1] G. Vetere, L. M. Tran, S. Moberg, P. E. Steadman, L. Restivo, F. G. Morrison, K. J. Ressler, S. A. Josselyn, P. W. Frankland, *Nat. Neurosci.* **2019**, *22*, 933.
[2] C. M. Bacmeister, R. Huang, L. A. Osso, M. A. Thornton, L. Conant, A. R. Chavez, A. Poleg-Polsky, E. G. Hughes, *Nat. Neurosci.* **2022**, *25*, 1300.
[3] S. A. Josselyn, S. Tonegawa, *Science* **2020**, *367*, eaaw4325.
[4] A. J. Doupe, P. K. Kuhl, *Annu. Rev. Neurosci.* **1999**, *22*, 567.
[5] W. Zhao, F. Garcia-Oscos, D. Dinh, T. F. Roberts, *Science* **2019**, *366*, 83.
[6] P. Smolen, Y. Zhang, J. H. Byrne, *Nat. Rev. Neurosci.* **2016**, *17*, 77.
[7] S. A. Josselyn, S. Kohler, P. W. Frankland, *Nat. Rev. Neurosci.* **2015**, *16*, 521.
[8] H. Eichenbaum, *Learn Behav* **2016**, *44*, 209.
[9] T. Wang, M. Wang, J. Wang, L. Yang, X. Ren, G. Song, S. Chen, Y. Yuan, R. Liu, L. Pan, Z. Li, W. R. Leow, Y. Lou, S. Ji, Z. Cui, K. He, F. Zhang, F. Lv, Y. Tian, K. Cai, B. Yang, J. Niu, H. Zou, S. Liu, G. Xu, X. Fan, B. Hu, X. J. Loh, L. Wang, X. Chen, *Nat. Electron.* **2022**, *5*, 586.
[10] Y. Kim, A. Chortos, W. Xu, Y. Liu, J. Y. Oh, D. Son, J. Kang, A. M. Foudeh, C. Zhu, Y. J Lee, S. Niu, J. Liu, R. Pfattner, Z. Bao, T.-W. Lee, *Science* **2018**, *360*, 998.
[11] A. Tahir, F. Chen, H. U. Khan, Z. Ming, A. Ahmad, S. Nazir, M. Shafiq, *Sensors* **2020**, *20*, 5392.
[12] A. R. Khan, M. Othman, S. A. Madani, S. U. Khan, *IEEE Commun. Surv. Tutor.* **2014**, *16*, 393.
[13] N. Nadimi, H. S. Lori, A. M. Amiri, *P. I. Civil. Eng-Transp.* **2021**, https://doi.org/10.1680/jtran.20.00128
[14] S. Behzadnia, S. Shahmohammadi, *J. Pediatr. Rev.* **2016**, *4*, e4780.
[15] A. Denoth-Lippuner, S. Jessberger, *Nat. Rev. Neurosci.* **2021**, *22*, 223.
[16] G. Hong, C. M. Lieber, *Nat. Rev. Neurosci.* **2019**, *20*, 330.
[17] J. Ma, J. Tang, *Nonlinear Dyn* **2017**, *89*, 1569.
[18] X. Hu, Z. Li, J. Chen, *Angew. Chem., Int. Ed.* **2017**, *56*, 5785.
[19] R. Wieduwild, S. Krishnan, K. Chwalek, A. Boden, M. Nowak, D. Drechsel, C. Werner, Y. Zhang, *Angew. Chem., Int. Ed.* **2015**, *127*, 4034.
[20] T. Chen, L. Qiu, Z. Yang, Z. Cai, J. Ren, H. Li, H. Lin, X. Sun, H. Peng, *Angew. Chem., Int. Ed.* **2012**, *51*, 11977.
[21] C. Tang, S. Xie, M. Wang, J. Feng, Z. Han, X. Wu, L. Wang, C. Chen, J. Wang, L. Jiang, P. Chen, X. Sun, H. Peng, *J. Mater. Chem. B* **2020**, *8*, 4387.
[22] I. M. Taylor, N. A. Patel, N. C. Freedman, E. Castagnola, X. T. Cui, *Anal. Chem.* **2019**, *91*, 12917.
[23] Y. Liu, J. Liu, S. Chen, T. Lei, Y. Kim, S. Niu, H. Wang, X. Wang, A. M. Foudeh, J. B.-H. Tok, Z. Bao, *Nat. Biomed. Eng.* **2019**, *3*, 58.
[24] J. Rivnay, H. Wang, L. Fenno, K. Deisseroth, G. G. Malliaras, *Sci. Adv.* **2017**, *3*, e1601649.
[25] G. Schiavone, X. Kang, F. Fallegger, J. Gandar, G. Courtine, S. P. Lacour, *Neuron* **2020**, *108*, 238.
[26] B. Zaaimi, M. Turnbull, A. Hazra, Y. Wang, C. Gandara, F. McLeod, E. E. McDermott, E. Escobedo-Cousin, A. Shah Idil, R. G. Bailey, S. Tardio, A. Patel, N. Ponon, J. Gausden, D. Walsh, F. Hutchings, M. Kaiser, M. O. Cunningham, G. J. Clowry, F. E. N. LeBeau, T. G. Constandinou, S. N. Baker, N. Donaldson, P. Degenaar, A. O'Neill, A. J. Trevelyan, A. Jackson, *Nat. Biomed. Eng.* **2022**, https://doi.org/10.1038/s41551-022-00945-8.
[27] K. Malpass, *Nat. Rev. Neurol.* **2013**, *9*,1.
[28] L. Gao, J. Wang, Y. Zhao, H. Li, M. Liu, J. Ding, H. Tian, S. Guan, Y. Fang, *Adv. Mater.* **2022**, *34*, 2107343.
[29] N. A. Steinmetz, C. Aydin, A. Lebedeva, M. Okun, M. Pachitariu, M. Bauza, M. Beau, J. Bhagat, C. Böhm, M. Broux, S. Chen, J. Colonell, R. J. Gardner, B. Karsh, F. Kloosterman, D. Kostadinov, C. Mora-Lopez, J. O'Callaghan, J. Park, J. Putzeys, B. Sauerbrei, R. J. J. van Daal, A. Z.

Vollan, S. Wang, M. Welkenhuysen, Z. Ye, J. T. Dudman, B. Dutta, A. W. Hantman, K. D. Harris, et al, *Science* **2021**, *372*, eabf4588.
[30] C. Stringer, M. Pachitariu, N. Steinmetz, C. B. Reddy, M. Carandini, K. D. Harris, *Science* **2019**, *364*, eaav7893.
[31] S. L. Metzger, J. R. Liu, D. A. Moses, M. E. Dougherty, M. P. Seaton, K. T. Littlejohn, J. Chartier, G. K. Anumanchipalli, A. Tu-Chan, K. Ganguly, E. F. Chang, *Nat. Commun.* **2022**, *13*, 6510.
[32] S. N. Flesher, J. E. Downey, J. M. Weiss, C. L. Hughes, A. J. Herrera, E. C. Tyler-Kabara, M. L. Boninger, J. L. Collinger, R. A. Gaunt, *Science* **2021**, *372*, 831.
[33] F. R. Willett, D. T. Avansino, L. R. Hochberg, J. M. Henderson, K. V. Shenoy, *Nature* **2021**, *593*, 249.
[34] S. Q. Lima, G. Miesenböck, *Cell* **2005**, *121*, 141.